Article

Diaryltin Dihydrides and Aryltin Trihydrides with Intriguing Stability

Beate G. Steller * [ORCID]**, Berenike Doler and Roland C. Fischer** [ORCID]

Graz University of Technology, Stremayrgasse 9/V, 8010 Graz, Austria; b.doler@student.tugraz.at (B.D.);
roland.fischer@tugraz.at (R.C.F.)

* Correspondence: beate.steller@tugraz.at

check for
updates

Abstract: In the last few decades, organotin hydrides have proven their potential as building blocks for a great variety of organometallic compounds. In this context, organotin hydrides with sterically shielding aryl substituents have attracted special interest, as these ligands can kinetically stabilize metastable products. The selective synthesis of aryltin halide compounds $Ar^*_2SnCl_2$ and Ar^*SnI_3 featuring the highly sterically encumbered aryl ligand Ar^* ($^{iPr}Ar^* = 2,6\text{-}(Ph_2CH)_2\text{-}4\text{-}iPrC_6H_2$; $^{Me}Ar^* = 2,6\text{-}(Ph_2CH)_2\text{-}4\text{-}MeC_6H_2$) is presented. These aryltin halides were converted into corresponding aryltin hydrides $Ar^*_2SnH_2$ and Ar^*SnH_3, which exhibit a surprisingly high thermal stability and oxygen tolerance.

Keywords: main group chemistry; tin hydrides; organotin chemistry; NMR spectroscopy; X-ray crystallography

1. Introduction

Compared to their carbon analogue, the element–hydrogen bond of heavier group 14 elements exhibits a far different stability and chemical behavior. [1] Thereby, the tin–hydrogen bond represents a fascinating border in group 14, as they show a wider range of possible reaction mechanisms than the corresponding germanium or silicon bond but are more readily accessible than lead hydrides [2,3]. While organotin hydrides R_nSnH_{4-n} are stable against moisture, they are usually thermolabile and readily react with oxygen to form the corresponding hydroxides or oxides. Their tolerance to oxygen and heat increases with increasing number of organic substituents and is additionally enhanced by organic substituents, which offer some steric protection [4]. Despite, or precisely because of, their labile nature, they have found wide application in organic synthetic chemistry, e.g., in hydrostannolysis and hydrostannation, as well as in organometallic chemistry as prominent starting materials for the synthesis of transition metal and main group compounds [5]. In the last few decades, (catalytic) dehydrogenative coupling of diorganotin diyhdrides has attracted wide interest in the preparation of oligo- and polystannanes [6–8]. More recent synthetic efforts have shown their intriguing reactivity and their potential as starting materials for corresponding low oxidation compounds, polyhedral cages and clusters or mixed-metal compounds (Figure 1).

The reactivity of tin hydrides was exploited in the reaction of an unsymmetrically substituted diaryltin dihydride $R'RSnH_2$ ($R' = Tbb = 2,6\text{-}[(Me_3Si)_2HC]_2\text{-}4\text{-}tBuC_6H_2$, $R = Mes = 2,4,6\text{-}Me_3C_6H_2$) with elemental sulfur to give access to a tetrathiastannolane [9]. Later $ArSnH_3$ ($Ar = 2,6\text{-}Tripp_2C_6H_3$; $Tripp = 2,4,6\text{-}iPr_3C_6H_2$) was converted with elemental sulfur to give a bicyclic tin/sulfur cage at elevated temperatures [10]. Tilley et al. obtained an $Os = Sn$ double bond by the reaction of an $TrippSnH_3$ and $Cp^*(iPr_3P)(H)Os(CH_2Ph)$ [11]. Similarly, a $Ru = Sn$ double bond was accessed from $Cp^*Ru(IXy\text{-}H)N_2$ ($IXy = 1,3\text{-}bis(2,6\text{-}dimethylphenyl)imidazol-2-ylidene$) using $TrippSnH_3$ as well [12]. The group of Wesemann performed reactivity studies of N-heterocyclic carbenes (NHCs) with diaryltin diyhdrides

and aryltin trihydrides. Products in these conversions do not only depend on the organic substituents on tin and the NHC, but also on stoichiometric ratios of tin hydride to applied NHC and the solvent. In the course of this work, access to NHC-stabilized low valent tin(II) compounds was granted starting from Tripp$_2$SnH$_2$ to give Tripp$_2$Sn(NHC) and from RSnH$_3$ to give RSnH(NHC) (R = Tripp, 2,6-Mes$_2$C$_6$H$_3$, 2,6-Tripp$_2$C$_6$H$_3$, (Me$_3$Si)$_2$CH) [13]. The low-valent species R$_2$Sn(NHC) turned out to be a convenient synthon for Pt, Pd and Ni containing distannametallacyclopropanes [14]. Moreover, neutral and charged metalloid clusters as well as NHC-stabilized Sn chains in variable length (2–4 tin atoms in a row) with two stannyl-stannylene sites have been obtained from dehydrogenative coupling of RSnH$_3$ (R = (Me$_3$Si)$_2$CH) [13,15]. Lately, reaction of a sterically encumbered ArSnH$_3$ (Ar = 2,6-TrippC$_6$H$_3$) with [Ph$_3$C][Al(OC{CF$_3$}$_3$)$_4$] gave an organodihydrostannylium salt [ArSnH$_2$][Al(OC{CF$_3$}$_3$)$_4$], which readily eliminates H$_2$ when warming up to room temperature and gives the low valent organotin cation [ArSn]$^+$ [16]. Corresponding dihydridostannate anions were obtained by deprotonation of the same aryltin trihydride using lithium diisopropylamide (LDA). This organodihydridostannate reacts as a nucleophile with low valent group 14 electrophiles [17] and with metallocene dichlorides of Ti, Zr and Hf to give corresponding metallocene bis(hydridoorgano-stannylene) complexes [18].
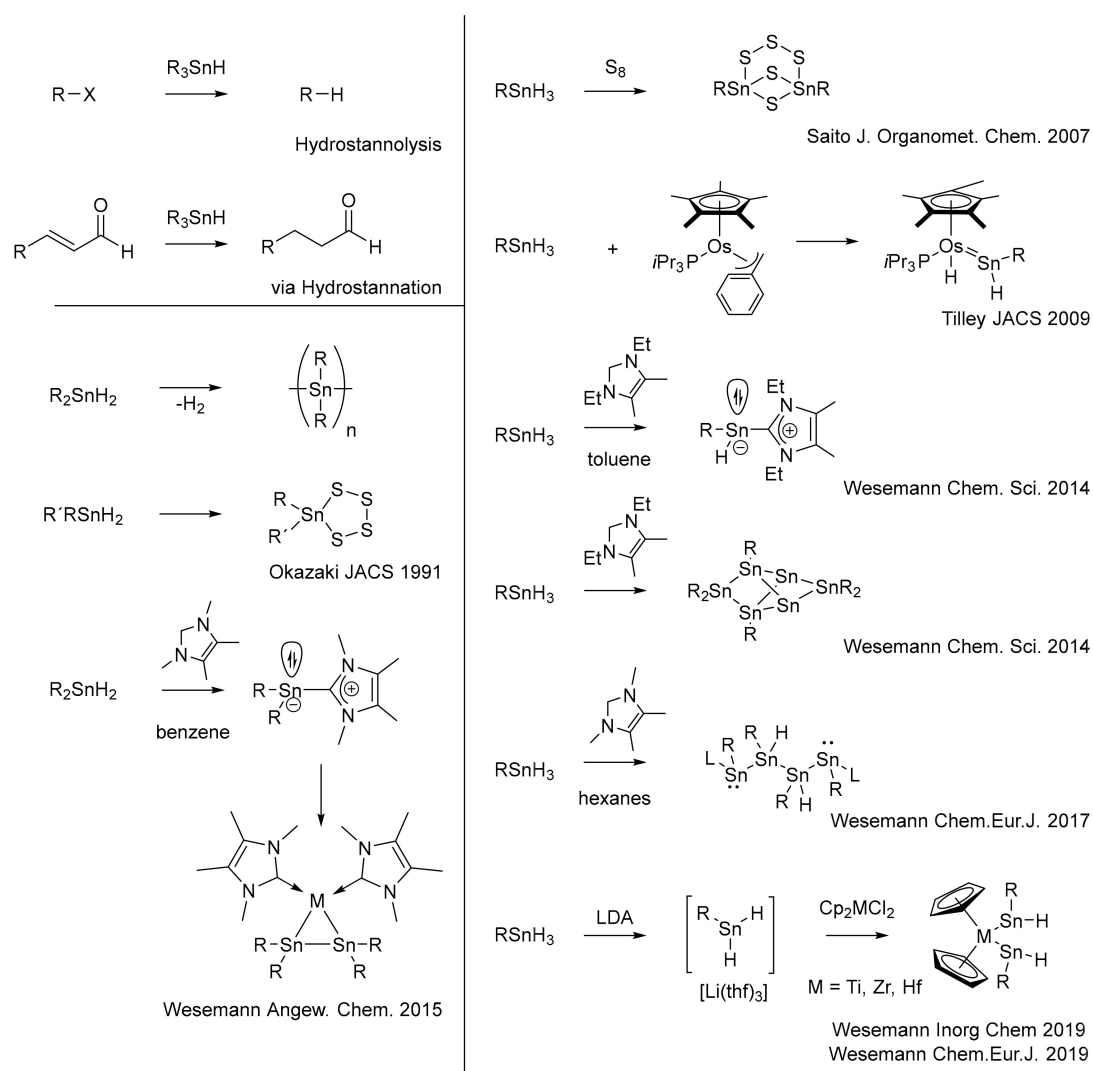

Figure 1. Organotin hydrides and their applications and reactivities.

The first successfully isolated organotin hydride, Me$_3$SnH, was accessed by treatment of the corresponding organotin sodium compound with ammonium chloride in liquid ammonia [19]. Still, after these initial investigations, tin hydrides were nearly neglected due to their challenging and

specific synthesis and instability, until Finholt and co-workers applied $LiAlH_4$ to generate SnH_4, $MeSnH_3$, Me_2SnH_2 and Me_3SnH from the corresponding chlorides next to other group 14 element hydride compounds [20]. In a similar fashion, a range of organotin hydrides were accessed utilizing DIBAL-H as the hydride transfer reagent shortly afterwards [21]. Nevertheless, organotin hydrides are still usually accessed via the straightforward hydride transfer of the corresponding tin halide using $LiAlH_4$. More rarely, other metal hydrides like $NaBH_4$, LiH, $(MeSiHO)_n$, Et_3SiH, R_3SnH are utilized[4]. Therefore, once the organotin halides are in hand, the corresponding hydrides are readily available.

Herein, we report the synthesis of diaryltin dihalides and aryltin trihalides and corresponding hydrides featuring a recently introduced bulky ligand backbone Ar* (^{iPr}Ar* = 2,6-$(Ph_2CH)_2$-4-$iPrC_6H_2$; ^{Me}Ar* = 2,6-$(Ph_2CH)_2$-4-MeC_6H_2) starting from the corresponding arly iodine Ar*I [22]. From the direct salt metathesis of in-situ prepared aryllithium solutions and $SnCl_4$, we were able to isolate solely the diaryltin dichloride $Ar*_2SnCl_2$ after recrystallization in good yields. In contrast, analytically pure aryltin triiodide $Ar*SnI_3$ was formed in conversions of the same aryllithium species and $SnCl_2$ (in a stoichiometric ratio 1:1.1) and subsequent oxidative addition with I_2. Isolated aryltin halides were converted into the corresponding hydride species using $LiAlH_4$ for tin dihydrides and DIBAL-H for tin trihydride species. All isolated compounds were fully characterized by heteronuclear NMR and IR spectroscopy as well as single crystal X-ray diffraction.

2. Results

2.1. Synthesis and Spectroscopic Data

Due to their sterically demanding carbon backbone, anilines $Ar*NH_2$ (Ar* = 2,6-$(Ph_2CH)_2$-4-R-C_6H_2, R = e.g., Me, iPr) have been applied as sterically shielding amide ligands for low oxidation state group 14 compounds [23–25]. Just recently, corresponding Ar*I was isolated and applied in the synthesis of sterically encumbered primary phosphanes [22]. Nevertheless, activation of the rather acidic C-H bond in the $CHPh_2$ moiety is likely to happen [26]. Possible modification of this ligand backbone and hence substitution of the rather acidic C-H in the $CHPh_2$ moiety was just recently displayed [27]. In order to rule out potential metalation of the rather benzylic C-H bond by lithium organyls, the targeted synthesis of Ar*Li was first conducted. Treatment of solutions of ^{iPr}Ar*I (**1**) or ^{Me}Ar*I (**2**) in toluene with stoichiometric amounts of nBuLi led to precipitation of ^{iPr}Ar*Li (**3**) and ^{Me}Ar*Li (**4**), respectively, from these solutions. Recrystallization of these powders from Et_2O gave crystals suitable for X-ray crystallography. NMR data as well as solid state structures corroborated lithiation of Ar*I by metal–halogen exchange rather than metalation of the C-H bond.

Therefore, synthesis of desired aryltin dichlorides **5** and **6** turned out the be straightforward. Following known procedures [28], the aryl iodides **1** and **2** were individually treated with a slight excess of nBuLi (1.15 eq) in Et_2O at low temperatures, followed by subsequent addition of $SnCl_4$ (0.5 eq) at low temperatures. Mixtures of halide species Ar_2SnCl_2, Ar_2SnICl and Ar_2SnI_2 were expected in crude products [28]. Nevertheless, NMR investigations of the crude product after extraction of an aliquot with $CDCl_3$ revealed the formation of mainly one tin species (see Supplementary Materials; p S2, Figures S1 and S2). In agreement with literature values, the main products were first identified to be $Ar*_2SnCl_2$ **5** and **6**, which was later confirmed by X-ray crystallography (Figure 2). In contrast to Molloy et al. [28], who observed the sole formation of the corresponding distannane $BrAr_2SnSnAr_2Br$ when using the less sterically hindered carbanion 2,4,6-$iPr_3C_6H_2Li$ with $SnBr_4$ in THF, we were not able to identify significant amounts of distannane in crude products with the highly sterically crowded Ar*Li.
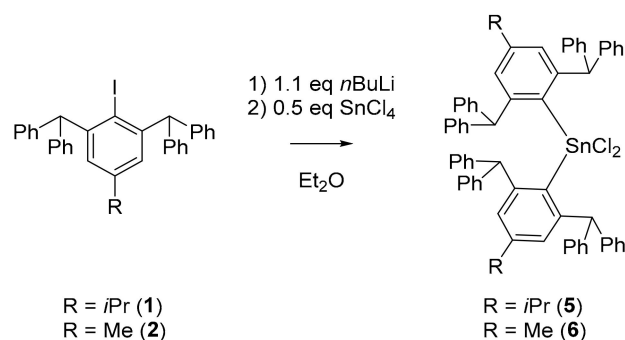
Figure 2. Synthesis of ^{iPr}Ar*$_2$SnCl$_2$ (**5**) and ^{Me}Ar*$_2$SnCl$_2$ (**6**) from ^{iPr}Ar*I (**1**) and ^{Me}Ar*I (**2**), respectively.

Synthesis of the corresponding aryltin trihalides by simply adjusting the stoichiometric ratio of Ar*Li and SnCl$_4$ was unsuccessful. Interestingly, reactions with a Ar*Li:SnCl$_4$ ratio of 0.9:1 and slow addition of the aryllithium species to SnCl$_4$ in Et$_2$O at low temperature yielded again Ar*$_2$SnCl$_2$ as the main product alongside unreacted SnCl$_4$. Similar results were also observed when changing the solvent to THF or toluene. As an alternative synthetic method [29,30], the reaction of ^{iPr}Ar*SnMe$_3$ (**7**), obtained from conversions of ^{iPr}Ar*Li with Me$_3$SnCl, with an excess of tin tetrachloride was investigated (Figure 3). Yet, even after prolonged reaction times and high excess of SnCl$_4$, only the dichloride ^{iPr}Ar*SnCl$_2$Me (**8**) was isolated from these approaches. Also, addition of catalytic amounts of AlCl$_3$ did not lead to the transfer of the remaining methyl group and formation of the desired ^{iPr}ArSnCl$_3$. Inspired by the synthesis of an ArSnI$_2$Cl (Ar = 2,6-(Me$_2$NCH$_2$)$_2$C$_6$H$_3$) from ArSnCl and I$_2$ [31], stoichiometric amounts of Ar*SnX (X = Cl, I), prepared in situ from Ar*Li and SnCl$_2$ (1:1), and I$_2$ were converted in order to yield an aryltin trihalide. The fading purple color after addition of I$_2$ indicated an already ongoing reaction. Finally, analytically pure aryltin triiodide species **9** and **10** were obtained (68 and 53%) from these reactions after recrystallization from toluene/*n*-heptane and DCM/*n*-heptane, respectively. Interestingly, in these approaches, again no mixtures of halide species Ar*SnX$_3$ (X = Cl or I) were observed in crude products, while a second tin species present in crude products with a highly lowfield-shifted resonance was assigned to be Ar*$_2$SnI$_2$ (for ^{iPr}Ar*: δ = −498 ppm; for ^{Me}Ar*: δ = −496 ppm) in agreement with literature values [32] (see Supplementary Materials, p S3, Figure S3). Conversion of an aliquot of such a crude product gained in the synthesis of **9** with LiAlH$_4$ and subsequent NMR investigation of reaction solutions revealed the formation of small amounts of ^{iPr}Ar*$_2$SnH$_2$ (**11**), as the expected product from the corresponding tin halide present in the mixture, next to the main product ^{iPr}Ar*SnH$_3$ (**13**) (see Supplementary Materials, p S3, Figure S4). These products were identified based on NMR data similar to literature values and later corroborated by the synthesis of **11** and **13**. Formation of Ar*$_2$SnI$_2$ was almost prevented when using a small excess of SnCl$_2$ in the first step of this synthesis (see Supplementary Materials, p S4, Figure S5).
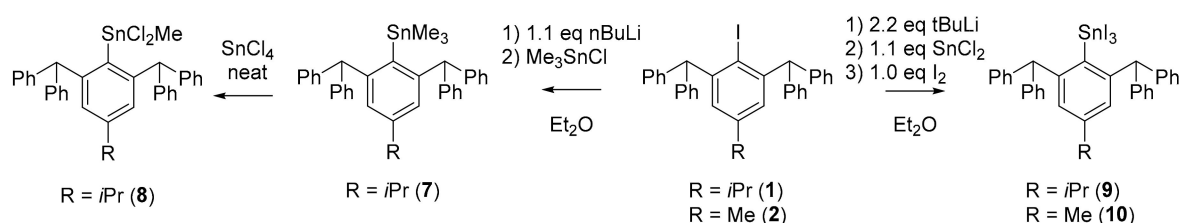
Figure 3. Preparation of arlytin compounds **7** and **8** as well as aryltin triioides **9** and **10**.

Diaryltin dihydrides **11** and **12** were accessed via the widely applied hydride transfer with LiAlH$_4$ of the corresponding chlorides **5** and **6** and subsequent aqueous work-up with degassed dilute H$_2$SO$_4$. Reactions were carried out in a solvent mixture of Et$_2$O/toluene due to low solubility of **5** and **6** in Et$_2$O alone. (Figure 4) After recrystallization from toluene/*n*-pentane, **11** and **12** were isolated in fair yields (50% and 53% respectively).

Figure 4. Hydrogenation of diaryltin dichlorides **5** and **6** utilizing LiAlH$_4$ leads to corresponding diaryltin dihydrides **11** and **12**, respectively.

When applying the same synthetic protocol in conversions of **9** and **10** to corresponding aryltin trihydrides, even during short reaction times the formation of a grey solid—presumably elemental tin—was observed. From these reactions only grey, nearly black, crude products were isolated with the desired aryltin tri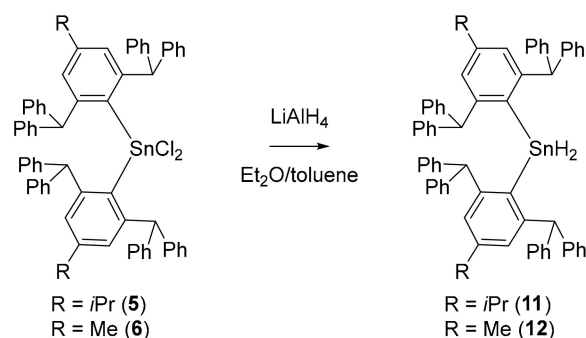hydrides **13** and **14** in only up to 70% purity. Hydrolyzed ligand Ar*H was identified as the main byproduct by ^{1}H NMR. In reactions with LiAlH$_4$ neither the use of substoichiometric amounts of LiAlH$_4$ nor omitting the common aqueous work-up could improve these results. Yet, utilization of DIBAL-H instead of LiAlH$_4$ as a softer hydride transfer agent gave satisfying results. After removal of all volatiles under reduced pressure and extraction of the resulting solid with *n*-pentane to remove byproducts and excess of DIBAL-H, **13** and **14** were isolated in satisfying yields (50% and 56% respectively). (Figure 5) In contrast to corresponding halide compounds, aryltin hydrides are sensitive to oxygen and easily react with traces to give corresponding hydroxide and oxide compounds. Yet, their tolerance against oxygen and temperature can be significantly increased by the steric demand of the substituting ligands[4]. Isolated diaryltin dihydrides **11** and **12** can be handled for a short period in air and possess an extraordinary thermal stability with melting points up to 200 °C. Likewise, isolated trihydrides **13** and **14** featuring this sterically crowded ligand Ar* possess astonishingly increased decomposition temperatures of up to 100 °C, while the parent PhSnH$_3$ slowly decomposes even at low temperatures [21].
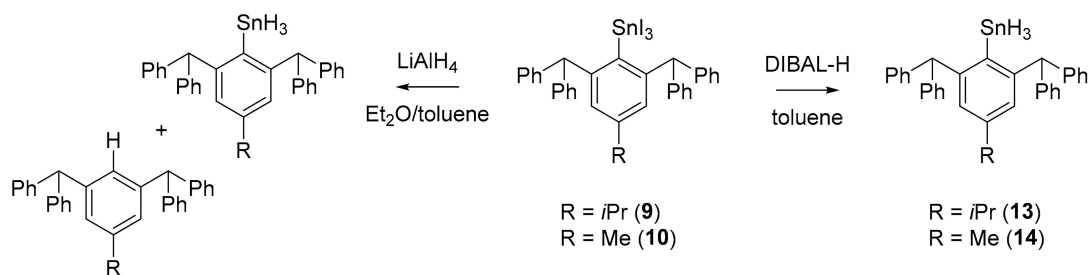
Figure 5. Hydrogenation of aryltin triiodies **9** and **10** with LiAlH$_4$ leads to a mixture of the corresponding hydride and hydrolyzed ligand. Using a softer hydride transfer reagent like DIBAL-H gives access to **13** and **14**.

In agreement with literature values [32], ^{119}Sn NMR shifts of isolated diaryltin dichlorides [−65.96 (**5**), −64.65 (**6**) ppm] are shifted ca. 40 ppm upfield compared to sterically less shielded diphenyltin dichloride (δ = −26.4 ppm). Yet, substitution of an aryl ligand by a methyl group results in a roughly 80 ppm downfield-shifted signal, as exemplified by resonances of Ph$_2$SnCl$_2$ [33] (−26.4 ppm) and PhSnMeCl$_2$ [34] (55.53 ppm) and here again observed for **5** (−65.96 ppm) and **8** (15.07 ppm). Nevertheless, the highly upfield-shifted resonances of corresponding diaryltin diiodides (−498.22 and −496.98, respectively; found in crude products of Ar*SnI$_3$) demonstrate a much stronger dependence on the nature of halide substituents, which is in full agreement with literature [32]. Even higher shifted

resonances are observed for aryltin triiodides **9** and **10** (−937.27 and −939.57 ppm, respectively). Again, this agrees with NMR shifts for $PhSnI_3$ [35] (−699.9 ppm) and $Ar^{CN}SnI_3$ [36] (−944.38 ppm).

^{119}Sn NMR resonances and coupling constants of isolated tin hydrides are in full agreement with literature data. Resonances of shifts of diaryltin dihydrides **11** (−331.30 ppm) and **12** (−331.51 ppm) are shifted by ca. 100 ppm upfield compared to parent Ph_2SnH_2. Therefore, these values agree with resonances for species with less sterically demanding *ortho*-alkyl groups of the aryl substituents, e.g., $Tripp_2SnH_2$ [13] (Tripp = 2,4,6-*i*$Pr_3C_6H_2$; −351.2 ppm). Substitution of an aryl group by a hydride leads to an upfield-shifted resonance for **13** (−406.06 ppm) and **14** (−406.67 ppm). These values are consistent with ^{119}Sn NMR shifts found for $TrippSnH_3$ (−416 ppm) and (2,6-$Tripp_2C_6H_3$)SnH_3 (−384.7 ppm). An summary of spectroscopic data is provided in Table 1.

Table 1. Sn NMR shifts (ppm) of aryltin compounds and ^{119}Sn NMR shifts (ppm) and coupling constants (Hz) of isolated aryltin hydrides.

	^{119}Sn NMR (ppm)	^{119}Sn NMR (ppm)	^{119}Sn NMR (ppm)	^1J (^{1}H, $^{117/119}$Sn) (Hz)
	X = Cl	X = I	X = H	
$^{iPr}Ar^*_2SnX_2$	−65.96	−498.22 *	−331.30	1942/2033
$^{Me}Ar^*_2SnX_2$	−64.65	−496.98 *	−331.51	1930/2019
$^{iPr}Ar^*SnMe_3$	−56.80	-	-	-
$^{iPr}Ar^*SnMeX_2$	+15.07	-	-	-
$^{iPr}Ar^*SnX_3$	-	−937.27	−407.06	1843/1930
$^{Me}Ar^*SnX_3$	-	−939.57	−406.67	1845/1931

Signals marked with * were only found in crude products.

2.2. Solid State Structures

All isolated arlytin halides and hydrides have been structurally characterized by X-ray crystallography. An overview of selected bond lengths and angles of isolated aryltin halides **5**, **6, 8, 9** as well as **10** is provided in Table 2. Irrespective of the substituent or number of aryl substituents, the tin atom is found in a distorted tetrahedral environment (Figure 6). The C-Sn-C angles of diaryltin dichlorides **5** (125.77(7)°) and **6** (119.5(2)°) are widened and deviate significantly from the ideal tetrahedral geometry. Therefore, Cl-Sn-Cl angles (94.49(3)° for **5** and 95.82(5) ° for **6**) are sharper than in less sterically crowded Ph_2SnCl_2 [37] (101.7(1)°) or Mes_2SnCl_2 [38] (Mes = 2,4,6-$Me_3C_6H_2$; 100.29(7)°), but are in agreement with diaryltin dichlorides featuring aryl groups with bulky *ortho*-substituents, e.g., $Tripp_2SnCl_2$ [39] (120.4(2)°) and $Mes^*_2SnCl_2$ [40] (Mes* = 2,4,6-*t*$Bu_3C_6H_2$; 95.5(1)°). A similar acute C-Sn-C angle is observed in **8** (92.47(7)°) despite the reduced sterical demand of the methyl substituent compared to a second $^{iPr}Ar^*$ substituent. The Sn-C^{Ar} bond length of **8** (2.140(6) and 2.141(7) Å, two independent molecules in the asymmetric unit) is slightly elongated compared to Ph_2SnCl_2 (2.112(5) Å). Likewise, Sn-C bonds of **5** (2.1501(5) Å) and **6** (2.155(5) and 2.159(6) Å) are elongated compared to diaryltin dichlorides with no or less sterically demanding *ortho*-alkyl groups of the aryl subsitutent, e.g., Ph_2SnCl_2 (2.112(5) Å) and Mes_2SnCl_2 (2.117(2) Å), but agree with values of sterically encumbered $Mes^*_2SnCl_2$. Similar Sn-C bond lengths are found in aryltin triiodides **9** (2.161(2) Å) and **10** (2.158(3) Å). Notably, **9** and **10** represent, next to recently reported $Ar^{CN}SnI_3$ (Ar^{CN} = 2-(Me_2NCH_2)C_6H_4), the only structurally authenticated aryltin triiodides, so far [36]. In general, the number of organotin triiodides is limited to a total number of thirteen including various structures of alkyltin triiodides $MeSnI_3$ and $EtSnI_3$ coordinated by different Lewis bases [41]. The Sn-C bond values for **9** and **10** are elongated compared to corresponding bonds in $Ar^{CN}SnI_3$ (2.136(4) Å) and (2,6-$Mes_2C_6H_3$)$SnCl_3$ [42] (2.128(5) Å), but show similar values as in (2,6-$Tripp_2C_6H_3$)$SnCl_3$ [43] (2.154(5) Å). Average Sn-I bond lengths of **9** and **10** are shorter than in the molecular structure of $Ar^{CN}SnI_3$, a 5-fold coordinated tin species additionally coordinated by the amino functionality on the attached ligand. Average values for X-Sn-X angles in **9** (97.31(1) to 107.66(1)°) and **10** (95.665(12) to 105.743(11)°) are wider as in $Ar^{CN}SnI_3$

(92.693(12) to 110.641(13)°) and aryltin trichlorides (2,6-Mes$_2$C$_6$H$_3$)SnCl$_3$ (97.48(8) to 102.95(9)°) and (2,6-Tripp$_2$C$_6$H$_3$)SnCl$_3$ (98.12(6) to 102.96(7)°). Presumably due to the steric demand of the ligand, there is a total absence of any intermolecular interaction between X···Sn in **5, 6, 8, 9** as well as **10**.

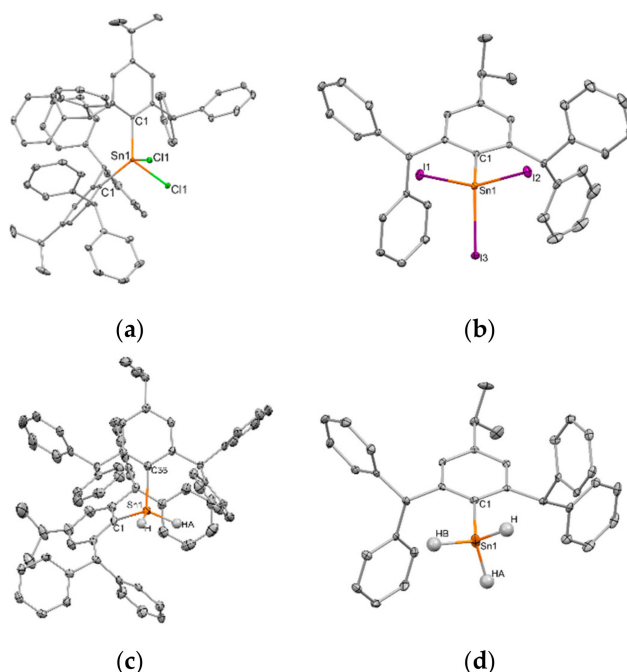(a)　　　　　　　　　　　　　　　　　　　　　(b)

(c)　　　　　　　　　　　　　　　　　　　　　(d)

Figure 6. Solid state structures of (**a**) **5**, (**b**) **9** and their corresponding tin hydride compounds (**c**) **11**, (**d**) **13**. All nonhydrogen atoms shown as 30% shaded ellipsoids. Hydrogen atoms except for those bonded to Sn are omitted for clarity. Selected bond lengths (Å) and angles (°) are displayed in Tables 2 and 3.

Table 2. Selected bond lengths (Å) and angles (°) of aryltin compounds **5, 6, 7, 8, 9** as well as **10** (X = Cl, I).

	Sn-C (Å)	Sn-X (Å)	C-Sn-C (°)	X-Sn-X (°)
^{iPr}Ar*$_2$SnCl$_2$ (**5**)	2.1501(15)	2.3781(5)	125.77(7)	94.49(3)
^{Me}Ar*$_2$SnCl$_2$ (**6**)	2.155(5), 2.159(6)	2.402(2), 2.344(2)	119.5(2)	95.82(5)
^{iPr}Ar*SnMe$_3$ (**7**)	2.189(1)	-	113.04(6) 111.75(6) 114.81(6)	-
^{iPr}Ar*SnMeCl$_2$ (**8**)	2.141(7) 2.140(6)	2.373(2), 2.375(2), 2.369(2) 2.381(2)	131.2(3) 130.0(3)	92.47(7)
^{iPr}Ar*SnI$_3$ (**9**)	2.161(2)	2.7130(4), 2.6964(4), 2.6721(4)	-	97.31(1), 106.04(1), 107.66(1)
^{Me}Ar*SnI$_3$ (**10**)	2.158(3)	2.6994(4), 2.6752(4)	-	105.743(11), 95.665(12)

Due to their high reactivity towards oxygen, the number of aryltin hydride compounds, which were structurally authenticated, is low, including only the structures of Ph$_2$SnH$_2$ [44] (crystallized from an in-situ technique in a capillary), Mes$_2$SnH$_2$ [45], Dep$_2$SnH$_2$ (Dep = 2, 6-Et$_2$C$_6$H$_2$), Dipp$_2$SnH$_2$ (Dipp = 2, 6-iPr$_2$C$_6$H$_2$) as well as Tripp$_2$SnH$_2$ [32] and in the case of aryltin trihydrides is limited to the structures of TrippSnH$_3$ [13] and (2,6-Tripp$_2$C$_6$H$_3$)SnH$_3$ [46]. Similar to all isolated aryltin halides, corresponding hydride compounds are found in a distorted tetrahedral environment (Figure 6). Selected bond lengths of **11** and **12** are summarized in Table 3. The Sn-C bonds in tin hydrides **11**

(2.187(3) and 2.171(3) Å) and **12** (12.188(2) and 2.186(2) Å) are elongated compared to corresponding distances in diaryltin dichlorides **5** and **6**. Yet, such a trend is not observed for **13** (2.1538(2) Å) and **14** (2.167(3) Å) and their corresponding aryltin triiodides **9** (2.161(2) Å) and **10** (1.58(3) Å). The C-Sn-C angles of **11** (105.9(1)°) and **12** (109.49(8)°) are more acute by approximately 20° and 10°, respectively, than in corresponding chlorides. All values found for isolated diaryltin dihydrides correspond to compounds with no or less sterically demanding *ortho*-alkyl groups of the aryl substituents, e.g., Ph_2SnH_2 and Mes_2SnH_2. Yet, no trend between steric demand of the aryl moiety and H-Sn-H as well as C-Sn-C angles is observed.

Table 3. Selected bond lengths (Å) and angles (°) of diaryltin dihydride compounds **11** and **12**.

	Sn-C (Å)	Sn-H (Å)	C-Sn-C (°)	H-Sn-H (°)
$^{iPr}Ar^*{}_2SnH_2$ (**11**)	2.187(3), 2.171(3)	1.71(3), 1.70(4)	105.9(1)	109(2)
$^{Me}Ar^*{}_2SnH_2$ (**12**)	2.188(2), 2.186(2)	1.79(2), 1.80(3)	109.49(8)	100.7(9)

3. Materials and Methods

All manipulations involving air or moisture sensitive compounds were either performed under a nitrogen atmosphere using standard Schlenk tube techniques or were carried out in a nitrogen flushed Glovebox UNILAB supplied by M. Braun. ^{1}H (300.22 MHz), ^{13}C (75.5 MHz), ^{7}Li (116.67 MHz) as well as ^{119}Sn (111.92 MHz) spectra were recorded on a Varian Mercury 300 MHz spectrometer from Varian. Spectra were referenced to solvent residual signals or with an external reference. Dried and deoxygenated solvents were obtained from an Innovative Technology solvent drying system. All other chemicals from commercial sources were used as purchased from chemical suppliers. $^{iPr}Ar^*NH_2$ and $^{Me}Ar^*NH_2$ ($^{iPr}Ar^* = 2,6\text{-}(Ph_2CH)_2\text{-}4\text{-}iPr\text{-}C_6H_2$; $^{Me}Ar^* = 2,6\text{-}(Ph_2CH)_2\text{-}4\text{-}Me\text{-}C_6H_2$) were synthesized following procedures described in the literature [47]. Corresponding Ar*I compounds were isolated from diazotization of the aniline Ar*NH$_2$ [22]. Elemental analysis was performed with an Elementar Vario MICRO cube. All IR measurements were measured fast under ambient conditions on an ALPHA-P device from Bruker in transmission mode. GC-MS measurements were carried out on an Agilent Technologies 7890A GC system coupled to an Agilent Technologies 5975 C VLMSD mass spectrometer using a HP5 column (30 m × 0.250 mm × 0.025 μm) and a carrier helium gas flow of 0.92726 mL/min. A 'hot needle' manual injection method at an injector temperature of 250 °C was performed. The MS conditions included positive EI ionization at ionization energy of 70 eV and a full scan mode (50–500 m/z). Melting points were determined by threefold determination with a Stuart SMP50 automatic melting point instrument.

For single crystal X-ray diffractometry, all suitable crystals were covered with a layer of silicone oil. A single crystal was selected, mounted on a glass rod on a copper pin, and placed in the cold N$_2$ stream provided by an Oxford Cryosystems cryometer (T = 100 K). XRD data collection was performed on a Bruker APEX II diffractometer with use of Mo Kα radiation (λ = 0.71073 Å) from an IμS microsource and a CCD area detector. Empirical absorption corrections were applied using SADABS [48,49]. The structures were solved with use of either direct methods or the Patterson option in SHELXS. Structure refinement was carried out using SHELXL [50,51]. CIF files were edited, validated and formatted with the program OLEX2 [52]. The space group assignments and structural solutions were evaluated using PLATON [53,54]. All nonhydrogen atoms were refined anisotropically. Hydrogen atoms next to the heavy atom Sn were located on the Fourier difference map in solid state structures of **11** and **12**. However, we were not able to locate hydrogens connected to Sn atoms in the Fourier difference map for **13** and **14**. Instead, hydrogen atoms were placed using a riding model for **13** as well as **14**. All other hydrogen atoms were placed in calculated positions corresponding to standard bond lengths and angles using riding models.

3.1. Synthesis

3.1.1. ^{iPr}Ar*I (**1**)

^{iPr}Ar*I was isolated from diazotization of the aniline ^{iPr}Ar*NH$_2$. [22] The crude product was recrystallized from acetone to give the product as a colorless solid.

Yield: 6.05 g (48%), colorless solid. m.p. 170-175 °C. Anal. Calcd. For C$_{35}$H$_{31}$I: C, 72.66; H, 5.40. Found: C, 72.66; H, 4.93. ^{1}H NMR (300.22 MHz, CDCl$_3$) δ 7.33-7.24 (m, 12 H; p/m-H^{Ar}(Ph), overlay with solvent peak), 7.10–7.08 (d, 8 H; o-H^{Ar}(Ph)), 6.69 (s, 2 H; o-H^{Ar}), 6.04 (s, 2 H; 2×CHPh$_2$), 2.66 (septet, ^{3}J$_{H,H}$ = 6.9 Hz, 1 H; CH(CH$_3$)$_2$), 1.01 (d, ^{3}J$_{H,H}$ = 6.9 Hz, 6 H; CH(CH$_3$)$_2$) ppm. ^{13}C NMR (75.5 MHz, CDCl$_3$) δ 147.85 (C^{Ar}), 147.16 (C^{Ar}), 143.45 (C^{Ar}(Ph)), 129.99 (C^{Ar}(Ph)), 128.37 (C^{Ar}(Ph)), 127.89 (C^{Ar}), 126.46 (C^{Ar}(Ph)), 108.26 (C^{Ar}-I), 62.21 (CHPh$_2$), 33.45 (CH(CH$_3$)$_2$), 23.76 (CH(CH$_3$)$_2$) ppm.

GC-MS (EI, 70 eV, toluene) t$_R$ = 23.689 min, m/z: 578.2 (M$^+$), 535.1 (M$^+$-CH(CH$_3$)$_2$), 451.3 (M$^+$-I).

3.1.2. ^{Me}Ar*I (**2**)

^{Me}Ar*I was isolated from diazotization of the aniline ^{iPr}Ar*NH$_2$. Spectroscopic data are in accordance with literature values. [22]

3.1.3. General Procedure for Ar*Li

In a Schlenk flask, aryl iodine was dissolved in toluene and cooled to −40 °C. At −40 °C, 1.1 eq of a nBuLi solution (1.7 M in hexanes) was added. After complete suspension, the solution was stirred at low temperatures for 1 h, while a colorless solid precipitated. The suspension was filtered, and the solid product was dried in vacuo. Crystals suitable for X-ray crystallography were obtained by recrystallization from Et$_2$O at −30 °C.

^{iPr}Ar*Li (**3**)

Here, 8.00 g **1** (13.8 mmol, 1.0 eq) and 8.8 mL nBuLi solution (1.7 M in hexanes, 15.2 mmol, 1.0 eq) in 150 mL were reacted according to the general procedure to yield a yellowish solid. The filtrate was concentrated and cooled to −30 °C to give a second crop.

Yield: 4.99 g (79%), yellowish powder. m.p. > 99 °C (decomposition). ^{1}H NMR (300.22 MHz, C$_6$D$_6$) δ 7.22–6.88 (m, 20 H; 20× o/m/p-H^{Ar}(Ph), overlay with solvent peak), 6.82 (s, 2 H; m-H^{Ar}), 6.05 (s, 2 H; 2×CHPh$_2$), 2.57 (sept, ^{3}J$_{H,H}$ = 6.9 Hz, 1 H; CH(CH$_3$)$_2$), 1.05 (d, ^{3}J$_{H,H}$ = 6.9 Hz, 6 H; CH(CH$_3$)$_2$) ppm. ^{13}C NMR (75.5 MHz, C$_6$D$_6$) δ 157.65 (C^{Ar}), 146.06 (C^{Ar}(Ph)), 129.93 (C^{Ar}(Ph)), 129.86 (C^{Ar}), 129.10 (C^{Ar}(Ph)), 126.81 (C^{Ar}(Ph)), 126.50 (C^{Ar}), 123.28 (C^{Ar}), 63.02 (CHPh$_2$), 34.34 (CH(CH$_3$)$_2$), 24.34 (CH(CH$_3$)$_2$) ppm. ^{7}Li NMR (116.67 MHz, C$_6$D$_6$) δ 1.77 ppm.

^{Me}Ar*Li (**4**)

Here, 2.97 g **2** (5.4 mmol, 1.0 eq) and 3.5 mL nBuLi solution (1.7 M in hexanes, 5.9 mmol, 1.1 eq) in 50 mL were reacted according to the general procedure to yield a yellowish powder.

Yield: 1.75 g (75%), yellowish powder. m.p. >94 °C (decomposition). ^{1}H NMR (300.22 MHz, C$_6$D$_6$) δ 7.21–6.88 (m, 20 H; o/m/p-H^{Ar}(Ph), overlay with solvent peak), 6.78 (s, 2 H; m-H^{Ar}), 6.08 (s, 2 H; 2×CHPh$_2$), 2.02 (s, 3 H; CH$_3$) ppm. ^{13}C NMR (75.5 MHz, C$_6$D$_6$) δ 158.02 (C^{Ar}), 145.91 (C^{Ar}(Ph)), 129.93 (C^{Ar}(Ph)), 129.87 (C^{Ar}), 129.13 (C^{Ar}(Ph)), 126.84 (C^{Ar}(Ph)), 126.50 (C^{Ar}), 125.94 (C^{Ar}), 62.93 (CHPh$_2$), 21.77 (CH$_3$) ppm. ^{7}Li NMR (116.67 MHz, C$_6$D$_6$) δ 1.84 ppm.

3.1.4. General Procedure for Ar*$_2$SnCl$_2$

A solution of nBuLi solution (1.7 M in hexanes) was added to a suspension of aryl iodine suspended in Et$_2$O at −50 °C. After full conversion was detected by GC-MS, the pale yellow solution was again cooled to −50 °C, SnCl$_4$ was added using a syringe. The reaction was allowed to warm up to rt overnight and the solvent was removed under reduced pressure. The resulting solid was extracted

twice with DCM and the solvent was again removed under reduced pressure to yield an off-white solid. The crude product was examined by ^{119}Sn NMR. For purification, the crude product was recrystallized from a mixture of DCM/*n*-pentane or DCM/toluene.

$^{i\text{Pr}}$Ar*$_2$SnCl$_2$ (**5**)

Here, 10.58 g **1** (18.3 mmol, 2.0 eq) in 150 mL, 12.1 mL *n*BuLi solution (1.7 M in hexanes, 20.6 mmol, 2.3 mmol) and 1.05 mL SnCl$_4$ (2.34 g, 9.0 mmol, 1.0 eq) were reacted according to the general procedure. The crude product was recrystallized from DCM/n-pentane. Crystals suitable for X-ray diffraction were obtained from recrystallization in DCM/*n*-heptane at −30 °C.

Yield: 6.26 g (63%), colorless solid. m.p. 247–251 °C. Anal. Calcd. for C$_{70}$H$_{62}$Cl$_2$Sn: C, 76.70; H, 5.49. Found: C, 75.97; H, 5.54. ^{1}H NMR (300.22 MHz, CDCl$_3$) δ 7.10–7.02 (m, 28 H; *p/m*-H^{Ar}(Ph) and *m*-H^{Ar}), 6.71 (d, 16 H, *o*-H^{Ar}(Ph)), 6.05 (s, 4 H; 4×C*H*Ph$_2$), 2.76 (sept, $^3J_{H,H}$ = 6.8 Hz, 2 H; 2×C*H*(CH$_3$)$_2$), 1.09 (d, $^3J_{H,H}$ = 6.8 Hz, 12 H; 2×CH(C*H*$_3$)$_2$) ppm. ^{13}C NMR (75.5 MHz, CDCl$_3$) δ 151.49 (C^{Ar}), 149.35 (C^{Ar}), 143.54 (C^{Ar}(Ph)), 142.78 (C^{Ar}), 129.87 (C^{Ar}(Ph)), 129.21 (C^{Ar}), 128.04 (C^{Ar}(Ph)), 126.41 (C^{Ar}), 58.11 (*C*HPh$_2$), 33.91 (*C*H(CH$_3$)$_2$) 23.74 (CH(*C*H$_3$)$_2$) ppm. ^{119}Sn NMR (111.92 MHz, CDCl$_3$) δ −65.96 ppm.

$^{\text{Me}}$Ar*$_2$SnCl$_2$ (**6**)

Here, 2.70 g **2** (4.90 mmol, 2.0 eq) in 50 mL, 3.20 mL *n*BuLi solution (1.7 M in hexanes, 5.44 mmol, 2.3 mmol) and 0.28 mL SnCl$_4$ (0.62 g, 2.40 mmol, 1.0 eq) were reacted according to the general procedure. The crude product was recrystallized from DCM/toluene. Crystals suitable for X-ray diffraction were obtained from recrystallization in DCM/*n*-heptane at rt.

Yield: 0.90 g (36%), colorless solid. m.p. 253–255 °C. Anal. Calcd. for C$_{66}$H$_{54}$Cl$_2$Sn: C, 76.46; H, 5.25. Found: C, 77.29; H, 5.65. ^{1}H NMR (300.22 MHz, CDCl$_3$) δ 7.12–7.01 (m, 24 H; *p/m*-H^{Ar}(Ph)), 6.91 (s, $^4J_{H,Sn}$ = 36.7 Hz, 4 H; *m*-H^{Ar}), 6.70 (d, 16 H; *o*-H^{Ar}(Ph)), 6.04 (s, 4 H; 4×C*H*Ph$_2$), 2.23 (s, 6 H; 2×C*H*$_3$) ppm. ^{13}C NMR (75.5 MHz, CDCl$_3$) δ 149.33 (C^{Ar}), 143.34 (C^{Ar}(Ph)), 142.54 (C^{Ar}), 140.89 (C^{Ar}), 131.75 (C^{Ar}), 129.87 (C^{Ar}(Ph)), 128.06 (C^{Ar}(Ph)), 126.42 (C^{Ar}(Ph)), 58.09 (*C*HPh$_2$) 21.88 (*C*H$_3$) ppm. ^{119}Sn NMR (111.92 MHz, CDCl$_3$) δ −64.65 ppm.

3.1.5. $^{i\text{Pr}}$Ar*SnMe$_3$ (**7**)

At −50 °C, 1.00 mL of a *n*BuLi solution (1.7 M in hexanes, 1.7 mmol, 1.1 eq) was added to a suspension of 0.91 g **1** (1.6 mmol, 1.0 eq) in 50 mL Et$_2$O. After full conversion was detected by GC-MS, 315 mg Me$_3$SnCl (1.6 mmol, 1.0 eq) were added. The reaction was allowed to warm up to rt, upon which a yellow solid was formed. For workup, the solvent was removed under reduced pressure and the gained solid was extracted with DCM (2 × 15 mL). The solvent was again removed under reduced pressure to give the pure product, which was used without further purification. Crystals suitable for single crystal X-ray diffraction were obtained by slow solvent evaporation from a solution in DCM.

Yield: 0.740 g (76%), yellow solid. m.p. 170–175 °C. ^{1}H NMR (300.22 MHz, CDCl$_3$) δ 7.31–7.19 (m, 12 H; *m/p*-H^{Ar}(Ph), overlay with solvent peak), 7.02 (d, $^3J_{H,H =}$ 7.0 Hz, 8 H; *o*-H^{Ar}(Ph)), 6.69 (s, $^4J_{H,H}$ = 16 Hz, 2 H; *m*-H^{Ar}), 5.92 (s, 2 H; 2×C*H*Ph$_2$), 2.64 (sept, $^3J_{H,H}$ = 6.9 Hz, 1 H; C*H*(CH$_3$)$_2$), 1.00 (d, $^3J_{H,H}$ = 6.9 Hz, 6 H; CH(C*H*$_3$)$_2$), 0.02 (s, $^2J_{H,Sn}$ = 52 Hz, 9 H; Sn(C*H*$_3$)$_3$) ppm. ^{13}C NMR (75.5 MHz, CDCl$_3$) δ 150.85 ($^2J_{C,Sn}$ = 31 Hz, C^{Ar}), 148.62 ($^4J_{C,Sn}$ = 9 Hz, C^{Ar}), 144.93 (C^{Ar}(Ph)), 142.15 (C^{Ar}), 130.08 (C^{Ar}(Ph)), 128.19 (C^{Ar}(Ph)), 126.71 (C^{Ar}), 126.32 (C^{Ar}(Ph)), 57.85 ($^3J_{C,Sn}$ = 30 Hz, *C*HPh$_2$), 33.73 (*C*H(CH$_3$)$_2$), 23.77 (CH(*C*H$_3$)$_2$), -4.17 ($^1J_{C,117Sn}$ = 326 Hz, $^1J_{C,119Sn}$ = 341 Hz; Sn(*C*H$_3$)$_3$) ppm. ^{119}Sn NMR (111.92 MHz, CDCl$_3$) δ −56.80 ppm.

3.1.6. $^{i\text{Pr}}$Ar*SnCl$_2$Me (**8**)

In a 50 mL Schlenk flask 620 mg **7** (1.0 mmol, 1.0 eq) was mixed neat with 0.15 mL SnCl$_4$ (335 mg, 1.3 mmol, 1.3 eq) and slowly heated up to 130 °C. The reaction was kept at 130 °C for 14 h. For workup the solid was extracted with DCM (6 mL), filtered and the solvent was removed under

reduced pressure. The crude product was recrystallized from DCM/*n*-pentane to give the compound in quantitative amounts. Crystals suitable for X-ray crystallography were obtained by recrystallization from DCM/*n*-heptane at rt.

Yield: 660 mg (quant.), colorless solid. m.p. 169–171 °C. ^{1}H NMR (300.22 MHz, CDCl$_3$) δ 7.33–7.22 (m, 12 H; *m/p*-H^{Ar}(Ph), overlay with solvent peak), 7.04 (d, ^{3}J = 6.9 Hz, 8 H; *o*-H^{Ar}(Ph)), 6.76 (s, ^{4}J = 10.5 Hz, 2 H; *m*-H^{Ar}), 6.63 (s, ^{4}J = 36.8 Hz, 2 H; 2×C*H*Ph$_2$), 2.76–2.54 (sept, ^{3}J$_{H,H}$ = 6.8 Hz, 1 H; C*H*(CH$_3$)$_2$), 0.97 (d, ^{3}J$_{H,H}$ = 6.8 Hz, 6 H; CH(C*H$_3$*)$_2$), -0.41 (s, ^{2}J$_{H,Sn}$ = 74.5 Hz, 3 H; SnCl$_2$(C*H$_3$*)) ppm. ^{13}C NMR (75.5 MHz, CDCl$_3$) δ 151.55 (C^{Ar}), 151.28 (C^{Ar}), 143.28 (C^{Ar}(Ph)), 130.83 (C^{Ar}(Ph)), 130.27 (C^{Ar}), 128.68 (C^{Ar}(Ph)), 127.48 (C^{Ar}), 127.19 (C^{Ar}(Ph)), 55.74 (^{3}J$_{C,Sn}$ = 39.4 Hz; *C*HPh$_2$), 33.93 (*C*H(CH$_3$)$_2$), 23.58 (CH(*C*H$_3$)$_2$), 6.20 (SnCl$_2$(*C*H$_3$)) ppm. ^{119}Sn NMR (111.92 MHz, CDCl$_3$) δ 15.07 ppm.

3.1.7. General Procedure for Ar*SnI$_3$

A solution of *t*BuLi (1.7 M in hexanes) was added to a suspension of aryl iodine suspended in Et$_2$O at −50 °C. After full conversion was detected by GC-MS, the pale yellow solution was again cooled to −50 °C and added in portions to a suspension of SnCl$_2$ in Et$_2$O also cooled to −50 °C. After complete addition, the reaction was allowed to warm up to rt overnight. At 0 °C, I$_2$ was added to the suspension upon which the suspension turned brownish. The reaction was allowed to warm up to rt and the color faded slowly to an intensive yellow. Volatiles were removed under reduced pressure and the resulting solid was extracted twice with DCM. The solvent was again removed under reduced pressure to yield an off-white solid. The crude product was examined by ^{119}Sn NMR. For purification, the crude product was recrystallized from a mixture of toluene/*n*-pentane or toluene.

$^{i\text{Pr}}$Ar*SnI$_3$ (**9**)

Here, 5.00 g **1** (8.64 mmol, 1.0 eq), 11.2 mL *t*BuLi solution (1.7 M in hexanes, 19.0 mmol, 2.2 eq), 1.80 g SnCl$_2$ (9.49 mmol, 1.1 eq) and 2.41 g I$_2$ (9.49 mmol, 1.1 eq) were reacted according to the general procedure. The crude product was recrystallized from toluene/*n*-pentane. Crystals suitable for X-ray diffraction were obtained from recrystallization in toluene/*n*-heptane at −30 °C.

Yield: 5.05 g (68%), yellow crystals. m.p. 181–183 °C. Anal. Calcd. for C$_{35}$H$_{31}$I$_3$Sn: C, 44.20; H, 3.29. Found: C, 43.37; H, 3.12. ^{1}H NMR (300.22 MHz, CDCl$_3$) δ 7.32–7.24 (m, 12 H; *p/m*-H^{Ar}(Ph), overlay with solvent peak), 7.05 (d, ^{3}J$_{H,H}$ = 6.6 Hz, 8 H; *o*-H^{Ar}(Ph)), 6.93 (s, ^{4}J$_{H,Sn}$ = 14.7 Hz, 2 H; *m*-H^{Ar}), 6.69 (s, ^{4}J$_{H,Sn}$ = 52.8 Hz, 2 H; 2×C*H*Ph$_2$), 2.73-2.64 (m, 1 H; C*H*(CH$_3$)$_2$), 0.99 (d, ^{3}J$_{H,H}$ = 6.9 Hz, 6 H; CH(C*H$_3$*)$_2$) ppm. ^{13}C NMR (75.5 MHz, CDCl$_3$) δ 152.33 (C^{Ar}), 149.94 (^{2}J$_{C,Sn}$ = 66.7 Hz; C^{Ar}), 143.05 (C^{Ar}(Ph)), 130.29 (C^{Ar}(Ph)), 129.10 (C^{Ar}), 129.01 (C^{Ar}), 128.56 (C^{Ar}(Ph)), 127.01 (C^{Ar}(Ph)), 55.45 (^{3}J$_{C,Sn}$ = 54.1 Hz; *C*HPh$_2$), 33.81 (*C*H(CH$_3$)$_2$), 23.56 (CH(*C*H$_3$)$_2$) ppm. ^{119}Sn NMR (111.92 MHz, CDCl$_3$) δ −937.27 ppm.

$^{\text{Me}}$Ar*SnI$_3$ (**10**)

Here, 4.08 g **2** (7.40 mmol, 1.0 eq), 9.6 mL *t*BuLi solution (1.7 M in hexanes, 16.3 mmol, 2.2 eq), 1.55 g SnCl$_2$ (8.16 mmol, 1.1 eq) and 2.07 g I$_2$ (8.16 mmol, 1.1 eq) were reacted according to the general procedure. The crude product was recrystallized from hot toluene. Crystals suitable for X-ray diffraction were obtained from recrystallization in DCM/*n*-heptane at −30 °C.

Yield: 3.68 g (53%), yellow crystals. m.p. 251–255 °C. Anal. Calcd. for C$_{33}$H$_{27}$I$_3$Sn: C, 42.94; H, 2.95. Found: C, 43.29; H, 2.83. ^{1}H NMR (300.22 MHz, CDCl$_3$) δ 7.34–7.24 (m, 12 H; *m/p*-H^{Ar}(Ph), overlay with solvent peak), 7.08 (d, ^{3}J$_{H,H}$ = 7.6 Hz, 8 H; *o*-H^{Ar}(Ph)), 6.93 (s, 2 H; *m*-H^{Ar}), 6.67 (s, 2 H; 2×C*H*Ph$_2$), 2.21 (s, 3 H; CH$_3$) ppm. ^{13}C NMR (75.5 MHz, CDCl$_3$) δ 149.80 (C^{Ar}), 142.96 (C^{Ar}(Ph)), 141.84 (C^{Ar}), 131.52 (C^{Ar}), 130.31 (C^{Ar}(Ph)), 128.81 (C^{Ar}), 128.58 (C^{Ar}(Ph)), 127.03 (C^{Ar}(Ph)), 55.34 (*C*HPh$_2$), 21.78 (*C*H$_3$) ppm. ^{119}Sn NMR (111.92 MHz, CDCl$_3$) δ −939.57 ppm.

3.1.8. General Procedure for Ar*$_2$SnH$_2$

In a Schlenk flask, LiAlH$_4$ was suspended in a mixture of Et$_2$O/toluene (4/1) and cooled down to 0 °C. At 0 °C, diaryltin dichloride was added. After 2 h of stirring at 0 °C, the reaction mixture was transferred via a cannula onto degassed H$_2$SO$_4$ (0.5 M, cooled to 0 °C), while anaerobic conditions were maintained. After separation of the layers, the organic phase was washed once with degassed, saturated potassium tartrate solution (75 mL) to remove aluminum salts, dried over Na$_2$SO$_4$ and filtered. The solvent was removed to give colorless crude reaction products.

$^{i\mathrm{Pr}}$Ar*$_2$SnH$_2$ (**11**)

Here, 82 mg LiAlH$_4$ (2.16 mmol, 1.2 eq) and 2.00 g **5** (1.83 mmol, 1.0 eq) were reacted according to the general procedure. The colorless crude product was recrystallized from toluene/n-pentane. Crystals suitable for X-ray crystallography were also obtained from a mixture of toluene/n-pentane at −30 °C.

Yield: 930 mg (50%), colorless crystals. m.p. 231–237 °C (decomposition at T > 250 °C). ^{1}H NMR (300.22 MHz, C$_6$D$_6$) δ 7.11–6.96 (m, 44 H; *o/m/p*-H$^{\mathrm{Ar}}$(Ph) and *m*-H$^{\mathrm{Ar}}$), 6.28 (s, 4 H; 4×C*H*Ph$_2$), 5.55 (s, $^{1}J_{\mathrm{H,117Sn}}$ = 1942 Hz, $^{1}J_{\mathrm{H,119Sn}}$ = 2033 Hz, 2 H; Sn*H*), 2.51 (sept, $^{3}J_{\mathrm{H,H}}$ = 6.8 Hz, 2 H; 2×C*H*(CH$_3$)$_2$), 0.99 (d, $^{3}J_{\mathrm{H,H}}$ = 6.8 Hz, 12 H; 2×CH(C*H*$_3$)$_2$) ppm. ^{13}C NMR (75.5 MHz, C$_6$D$_6$) δ 151.67 (C$^{\mathrm{Ar}}$), 149.84 (C$^{\mathrm{Ar}}$), 144.85 (C$^{\mathrm{Ar}}$(Ph)), 142.37 (C$^{\mathrm{Ar}}$), 130.47 (C$^{\mathrm{Ar}}$(Ph)), 128.51 (C$^{\mathrm{Ar}}$(Ph)), 127.45 (C$^{\mathrm{Ar}}$), 126.61 (C$^{\mathrm{Ar}}$(Ph)), 60.11 (CHPh$_2$), 34.21 (CH(CH$_3$)$_2$), 23.98 (CH(CH$_3$)$_2$) ppm. ^{119}Sn NMR (111.92 MHz, C$_6$D$_6$) δ −331.30 ($^{1}J_{\mathrm{Sn,1H}}$ = 2033 Hz) ppm. ATR-FTIR 1885 (s; ν$_\mathrm{s}$ SnH) cm^{-1}.

$^{\mathrm{Me}}$Ar*$_2$SnH$_2$ (**12**)

Here, 88 mg LiAlH$_4$ (2.32 mmol, 0.8 eq) and 3.00 g **6** (2.89 mmol, 1.0 eq) were reacted according to the general procedure. The colorless crude product was recrystallized from toluene/n-pentane or toluene/Et$_2$O. Crystals suitable for X-ray crystallography were obtained from toluene at −30 °C.

Yield: 1.50 g (54%), colorless crystals. m.p. 207–211 °C (decomposition at T > 215 °C). ^{1}H NMR (300.22 MHz, C$_6$D$_6$) δ 7.07–6.95 (m, 44 H; *o/m/p*-H$^{\mathrm{Ar}}$(Ph) and *m*-H$^{\mathrm{Ar}}$), 6.28 (s, 4 H; 4×C*H*Ph$_2$), 5.60 (s, $^{1}J_{\mathrm{H,117Sn}}$ = 1930 Hz, $^{1}J_{\mathrm{H,119Sn}}$ = 2019 Hz, 2 H; Sn*H*), 1.87 (s, 6 H; 2×C*H*$_3$) ppm. ^{13}C NMR (75.5 MHz, C$_6$D$_6$) δ 151.78 (C$^{\mathrm{Ar}}$), 144.70 (C$^{\mathrm{Ar}}$(Ph)), 141.40 (C$^{\mathrm{Ar}}$), 139.08 (C$^{\mathrm{Ar}}$), 130.45 (C$^{\mathrm{Ar}}$(Ph)), 130.16 (C$^{\mathrm{Ar}}$), 128.56 (C$^{\mathrm{Ar}}$(Ph)), 126.61 (C$^{\mathrm{Ar}}$(Ph)), 60.18 (CHPh$_2$), 21.44 (CH$_3$) ppm. ^{119}Sn NMR (111.92 MHz, C$_6$D$_6$) δ −331.51 ($^{1}J_{\mathrm{Sn,1H}}$ = 2019 Hz) ppm. ATR-FTIR 1886 (s; ν$_\mathrm{s}$ SnH) cm^{-1}.

3.1.9. General Procedure for Ar*SnH$_3$

In a round-bottom Schlenk flask, aryltin triiodide was dissolved in toluene to give a yellow solution and cooled to 0 °C. At 0 °C, a solution of DIBAL-H (1.0 M in toluene) was added, upon which the solution turned slowly colorless. After 1 h of stirring at 0 °C, the solvent was removed under reduced pressure to give a colorless oil. The oil was extracted three times with *n*-pentane or Et$_2$O, while being cooled to 0 °C, and the remaining colorless product was dried in vacuo.

iPrAr*SnH$_3$ (**13**)

Here, 2.00 g **9** (2.10 mmol, 1.0 eq) and 6.9 mL DIBAL-H solution (1.0 M in toluene, 6.90 mmol, 3.3 eq) were reacted according to the general procedure. The *n*-pentane was concentrated to give a second crop. Crystals suitable for X-ray crystallography were obtained by recrystallization from *n*-pentane at −30 °C.

Yield: 650 mg (54%), colorless solid. m.p. > 105 °C (decomposition). ^{1}H NMR (300.22 MHz, C$_6$D$_6$) δ 7.11–6.98 (m, 22 H; *o/m/p*-H$^{\mathrm{Ar}}$(Ph) and *m*-H$^{\mathrm{Ar}}$), 5.99 (s, 2 H; 2×C*H*Ph$_2$), 4.82 (s, $^{1}J_{\mathrm{H,117Sn}}$ = 1843 Hz, $^{1}J_{\mathrm{H,119Sn}}$ = 1930 Hz, 3 H; Sn*H*), 2.44 (sept, $^{3}J_{\mathrm{H,H}}$ = 6.8 Hz, 1 H; C*H*(CH$_3$)$_2$), 0.92 (d, $^{3}J_{\mathrm{H,H}}$ = 6.8 Hz, 6 H; CH(C*H*$_3$)$_2$) ppm. ^{13}C NMR (75.5 MHz, C$_6$D$_6$) δ 152.15 (C$^{\mathrm{Ar}}$), 149.63 (C$^{\mathrm{Ar}}$), 144.39 (C$^{\mathrm{Ar}}$(Ph)), 137.00 (C$^{\mathrm{Ar}}$), 130.64 (C$^{\mathrm{Ar}}$(Ph)), 128.69 (C$^{\mathrm{Ar}}$(Ph)), 126.94 (C$^{\mathrm{Ar}}$), 126.73 (C$^{\mathrm{Ar}}$(Ph)), 60.60 (CHPh$_2$), 34.12

$(CH(CH_3)_2)$, 23.86 $(CH(CH_3)_2)$ ppm. ^{119}Sn NMR (111.92 MHz, C_6D_6) δ −407.06 ($^1J_{Sn,1H}$ = 1930 Hz) ppm. ATR-FTIR 1848 (s; ν_s SnH) cm^{-1}.

^{Me}Ar*SnH$_3$ (**14**)

Here, 2.00 g **10** (2.10 mmol, 1.0 eq) and 6.7 mL DIBAL-H solution (1.0 M in toluene, 6.70 mmol, 3.1 eq) were reacted according to the general procedure. The Et$_2$O was concentrated to give a second crop. Crystals suitable for X-ray crystallography were obtained by recrystallization from toluene at rt.

Yield: 667 mg (56%), colorless crystals. m.p. > 110 °C (decomposition). ^{1}H NMR (300.22 MHz, C_6D_6) δ 7.10–6.99 (m, 20 H; $o/m/p$-H^{Ar}(Ph)), 6.92 (s, $^4J_{H,Sn}$ = 19.8 Hz, 2 H; m-H^{Ar}) 5.98 (s, 2 H; 2×CHPh$_2$), 4.83 (s, s, $^1J_{H,117Sn}$ = 1845 Hz, $^1J_{H,119Sn}$ = 1931 Hz, 3 H; SnH), 1.82 (s, 3 H; 2×CH_3) ppm. ^{13}C NMR (75.5 MHz, C_6D_6)k δ 151.74 (C^{Ar}), 143.88 (C^{Ar}(Ph)), 138.49 (C^{Ar}), 136.09 (C^{Ar}), 130.21 (C^{Ar}(Ph)), 129.10 (C^{Ar}), 128.29(C^{Ar}(Ph)), 126.31 (C^{Ar}(Ph)), 60.09 (CHPh$_2$), 20.95 (CH$_3$) ppm. ^{119}Sn NMR (111.92 MHz, C_6D_6) δ −406.67 ($^1J_{Sn,1H}$ = 1931 Hz) ppm. ATR-FTIR 1854 (s; ν_s SnH) cm^{-1}.

4. Conclusions

The sterically encumbered tin halides Ar*$_2$SnCl$_2$ and Ar*SnI$_3$ as well as corresponding tin hydrides Ar*$_2$SnH$_2$ and Ar*SnH$_3$ featuring the bulky ligand backbone Ar* (^{iPr}Ar* = 2,6-(CHPh$_2$)$_2$-4-iPrC$_6$H$_2$; ^{Me}Ar* = 2,6-(CHPh$_2$)$_2$-4-MeC$_6$H$_2$) were prepared and characterized by multinuclear (^{1}H, ^{13}C, ^{119}Sn) NMR as well as IR spectroscopy. Additionally, solid state structures of all reported compounds were authenticated by single crystal X-ray diffraction. Isolated aryltin trihydrides possess a surprisingly increased thermal stability and oxygen tolerance compared to less sterically encumbered organotin hydrides. Due to their less labile but still functional nature, isolated aryltin hydrides are likely to undergo follow-up chemistry. Their intriguing reactivities are currently examined.

Supplementary Materials: The following are available online. ^{119}Sn NMR of crude products in the synthesis of **5**, **6**, **9** and **10** (Figure S1-S5). NMR spectra (^{1}H, ^{13}C and if applicable ^{7}Li and ^{119}Sn) of all unknown isolated compounds (**1**, **3-14**) (Figure S6-S47). ATR-IR of isolated tin hydrides **11**, **12**, **13** and **14** (Figure S48-S51) and Raman spectra of aryltin iodides **9** and **10** (Figure S53-S54). Tabulated crystallographic data and ORTEP plots for compounds **1**, **3-14**. CCDC 1983429 (for **1**), 1983430 (for **3**), 1983431 (for **4**), 1983432 (for **7**), 1983433 (for **6**), 1983434 (for **11**), 1983435 (for **8**), 1983436 (for **5**), 1983437 (for **14**), 1983438 (for **13**), 1983439 (for **12**), 1983440 (for **10**) and 1983441 (for **9**) contain the supplementary crystallographic data for this paper. These data can be obtained free of charge from The Cambridge Crystallographic Data Centre.

Author Contributions: B.G.S. and B.D. conducted experimental work and acquired spectroscopic data. R.C.F. conducted X-ray crystallography measurements and solved structures. B.G.S. and R.C.F. initiated the project, designed experiments and wrote the paper. All authors have read and agreed to the published version of the manuscript.

Conflicts of Interest: The authors declare no conflict of interest.

References

1. Rivard, E. Group 14 Inorganic Hydrocarbon Analogues. *Chem. Soc. Rev.* **2016**, *45*, 989–1003. [CrossRef]
2. Holleman, A.F.; Nils Wiberg, E.; Fischer, G. *Lehrbuch Der Anorganischen Chemie*; Walter de Gruyter: Berlin, Germanny, 2007. [CrossRef]
3. Aldridge, S.; Downs, A.J. Hydrides of the Main-Group Metals: New Variations on an Old Theme. *Chem. Rev.* **2001**, *101*, 3305–3365. [CrossRef]
4. Davies, A.G. Organotin Hydrides. In *Organotin Chemistry*; Wiley-VCH Verlag GmbH & Co.: Weinheim, Germany, 2004; pp. 245–265.
5. Elschenbroich, C. *Organometallchemie*; Badura, B., Schröder, H., Vetter, C., Eds.; Vieweg+Teubner: Wiesbaden, Germany, 2008. [CrossRef]
6. Braunstein, P.; Morise, X. Dehydrogenative Coupling of Hydrostannanes Catalyzed by Transition Metal Complexes. *Chem. Rev.* **2000**, *100*, 3542–3552. [CrossRef]

7.　Hill, M.S. Homocatenation of Metal and Metalloid Main Group Elements. In *Metal-Metal Bonding*; Parking, G., Ed.; Springer-Verlag: Berlin, Germany, 2010; Volume 136, pp. 189–216. [CrossRef]

8.　Caseri, W. Polystannanes: Processible Molecular Metals With. *Chem. Soc. Rev.* **2016**, *45*, 5187–5199. [CrossRef]

9.　Tokitoh, N.; Suzuki, H.; Matsumoto, T.; Matsuhashi, Y.; Okazaki, R.; Goto, M. 1,2,3,4,5-Tetrathiametallolanes of Group 14 Metals, RR′MS4 (M = Si, Ge, and Sn): Synthesis and Crystal Structures. *J. Am. Chem. Soc.* **1991**, *113*, 7047–7049. [CrossRef]

10.　Saito, M.; Hashimoto, H.; Tajima, T.; Ikeda, M. Synthesis and Structures of Polychalcogenadistannabicyclo[k.l.m]Alkanes. *J. Organomet. Chem.* **2007**, *692*, 2729–2735. [CrossRef]

11.　Hayes, P.G.; Gribble, C.W.; Waterman, R.; Tilley, T.D. A Hydrogen-Substituted Osmium Stannylene Complex: Isomerization to a Metallostannylene Complex via an Unusual α-Hydrogen Migration from Tin to Osmium. *J. Am. Chem. Soc.* **2009**, *131*, 4606–4607. [CrossRef]

12.　Liu, H.J.; Guihaumé, J.; Davin, T.; Raynaud, C.; Eisenstein, O.; Tilley, T.D. 1,2-Hydrogen Migration To a Saturated Ruthenium Complex Via Reversal of Electronic Properties for Tin in a Stannylene-To-Metallostannylene Conversion. *J. Am. Chem. Soc.* **2014**, *136*, 13991–13994. [CrossRef]

13.　Sindlinger, C.P.; Wesemann, L. Hydrogen Abstraction from Organotin Di- and Trihydrides by N-Heterocyclic Carbenes: A New Method for the Preparation of NHC Adducts to Tin(I) Species and Observation of an Isomer of a Hexastannabenzene Derivative [R6Sn6]. *Chem. Sci.* **2014**, *5*, 2739–2746. [CrossRef]

14.　Sindlinger, C.P.; Weiß, S.; Schubert, H.; Wesemann, L. Nickel-Triad Complexes of a Side-on Coordinating Distannene. *Angew. Chem.-Int. Ed.* **2015**, *54*, 4087–4091. [CrossRef] [PubMed]

15.　Maudrich, J.J.; Sindlinger, C.P.; Aicher, F.S.W.; Eichele, K.; Schubert, H.; Wesemann, L. Reductive Elimination of Hydrogen from Bis(Trimethylsilyl)Methyltin Trihydride and Mesityltin Trihydride. *Chem.-A Eur. J.* **2017**, *23*, 2192–2200. [CrossRef] [PubMed]

16.　Diab, F.; Aicher, F.S.W.; Sindlinger, C.P.; Eichele, K.; Schubert, H.; Wesemann, L. Reductive Elimination and Oxidative Addition of Hydrogen at Organostannylium and Organogermylium Cations. *Chem.-A Eur. J.* **2019**, *25*, 4426–4434. [CrossRef] [PubMed]

17.　Maudrich, J.J.; Diab, F.; Weiß, S.; Widemann, M.; Dema, T.; Schubert, H.; Krebs, K.M.; Eichele, K.; Wesemann, L. Deprotonation of Organogermanium and Organotin Trihydrides. *Inorg. Chem.* **2019**, *58*, 15758–15768. [CrossRef]

18.　Maudrich, J.J.; Widemann, M.; Diab, F.; Kern, R.H.; Sirsch, P.; Sindlinger, C.P.; Schubert, H.; Wesemann, L. Hydridoorganostannylene Coordination: Group 4 Metallocene Dichloride Reduction in Reaction with Organodihydridostannate Anions. *Chem.-A Eur. J.* **2019**, *25*, 16081–16087. [CrossRef]

19.　Kraus, C.A.; Greer, W.N. The Preparation and Properties of Trimethylstannane. *J. Am. Chem. Soc.* **1922**, *44*, 2629–2633. [CrossRef]

20.　Finholt, A.E.; Bond, A.C.; Wilzbach, K.E.; Schlesinger, H.I. The Preparation and Some Properties of Hydrides of Elements of the Fourth Group of the Periodic System and of Their Organic Derivatives. *J. Am. Chem. Soc.* **1947**, *69*, 2692–2696. [CrossRef]

21.　Neumann, W.P.; Niermann, H. Darstellung Von Organozinn-Mono-, -Di- Und -Tri-Hydriden. *Eur. J. Inorg. Chem.* **1962**, *653*, 164–172.

22.　Bresien, J.; Goicoechea, J.M.; Hinz, A.; Scharnhölz, M.T.; Schulz, A.; Suhrbier, T.; Villinger, A. Increasing Steric Demand through Flexible Bulk-Primary Phosphanes with 2,6-Bis(Benzhydryl)Phenyl Backbones. *Dalton Trans.* **2019**, *48*, 3786–3794. [CrossRef]

23.　Protchenko, A.V.; Birjkumar, K.H.; Dange, D.; Schwarz, A.D.; Vidovic, D.; Jones, C.; Kaltsoyannis, N.; Mountford, P.; Aldridge, S. A Stable Two-Coordinate Acyclic Silylene. *J. Am. Chem. Soc.* **2012**, *134*, 6500–6503. [CrossRef]

24.　Hadlington, T.J.; Hermann, M.; Li, J.; Frenking, G.; Jones, C. Activation of H2 by a Multiply Bonded Amido-Digermyne: Evidence for the Formation of a Hydrido-Germylene. *Angew. Chem. Int. Ed.* **2013**, *52*, 10199–10203. [CrossRef] [PubMed]

25.　Hadlington, T.J.; Hermann, M.; Frenking, G.; Jones, C. Low Coordinate Germanium(II) and Tin(II) Hydride Complexes: Efficient Catalysts for the Hydroboration of Carbonyl Compounds. *J. Am. Chem. Soc.* **2014**, *136*, 3028–3031. [CrossRef] [PubMed]

26.　De Bruin-Dickason, C.N.; Boutland, A.J.; Dange, D.; Deacon, G.B.; Jones, C. Redox Transmetallation Approaches to the Synthesis of Extremely Bulky Amido-Lanthanoid(II) and -Calcium(II) Complexes. *Dalton Trans.* **2018**, *47*, 9512–9520. [CrossRef] [PubMed]

27. Vrána, J.; Samsonov, M.A.; Němec, V.; Růžička, A. Access to the Most Sterically Crowded Anilines via Non-Catalysed C–C Coupling Reactions. *Chem. Commun.* **2020**, *56*, 2–5. [CrossRef]

28. Brown, P.; Mahon, M.F.; Molloy, K.C. Sterically Hindered Organotin Compounds II. Synthesis of the Organotin Halides (Mesityl)2SnXnY2-n, (Mesityl)SnXnY3-n and R4Sn2X2 (R = 2,4,6-IPr3C6H2, X = Cl, Y = Br). Crystal Structure of the Ditin Species (R2BrSn)2. *J. Organomet. Chem.* **1992**, *435*, 265–273. [CrossRef]

29. Elhamzaoui, H.; Jousseaume, B.; Toupance, T.; Allouchi, H. α,ω-Bis(Trialkynyltin) Compounds with a Linear or Cross-Shaped Spacer. *Organometallics* **2007**, *26*, 3908–3917. [CrossRef]

30. Prabusankar, G.; Jousseaume, B.; Toupance, T.; Allouchi, H. A Discrete Unsymmetrically Substituted Dihydrodioxadistannetane with Both H1 and Intramolecular H2μ2 Sulfonate Bondings. *J. Organomet. Chem.* **2008**, *693*, 3383–3386. [CrossRef]

31. Bouska, M.; Dostá, L.; Jirásko, R.; Růžička, A.; Jambor, R. Synthesis of [{2,6-(Me2NCH2)2C 6H3}Sn(OH)0]6: An N-Sn Coordinated Stannonic Acid. *Organometallics* **2009**, *28*, 4258–4261. [CrossRef]

32. Steller, B.G.; Fischer, R.C. Selective Preparation of Sterically Encumbered Diaryltin Dihalides from Grignard Reagents via Salt Metathesis and Halide Exchange. *Eur. J. Inorg. Chem.* **2019**, *2019*, 2591–2597. [CrossRef]

33. Zeppek, C.; Pichler, J.; Torvisco, A.; Flock, M.; Uhlig, F. Aryltin Chlorides and Hydrides: Preparation, Detailed NMR Studies and DFT Calculations. *J. Organomet. Chem.* **2013**, *740*, 41–49. [CrossRef]

34. Kapoor, R.N.; Apodaca, P.; Montes, M.; Gomez, F.D.; Pannell, K.H. Mixed Aryl-Alkyl Organotin Compounds, ArMeSnCl3-n (Ar = RC6H4, R = H, Ethyl, i-Propyl, t-Butyl; n-Hexyl, n-Octyl) and the Effect of R upon Antibiotic Activity. *Appl. Organomet. Chem.* **2005**, *19*, 518–522. [CrossRef]

35. Pejchal, V.; J, H.; Lyčka, A. 13C and 119Sn NMR Spectra of Some Monophenyltin(IV) Compounds. *Sci. Pap. Univ. Pardubice* **1996**, *2*, 35–46.

36. Novák, P.; Padělková, Z.; Císařová, I.; Kolářová, L.; Růžička, A.; Holeček, J. Structural Study of C,N-Chelated Monoorganotin(IV) Halides. *Appl. Organomet. Chem.* **2006**, *20*, 226–232. [CrossRef]

37. Greene, B.P.T.; Bryan, R.F. Crystal Structure of Dichloro(Diphenyl)Tin. *J. Chem. Soc.* **1971**, 2549–2554. [CrossRef]

38. Kräuter, T.; Neumüller, B. Die Kristallstrukturen von MesSn(Cl)Me2 Und Mes2SnCl2. *Zeitschrift für Naturforsch. B* **1998**, *53*, 503–506. [CrossRef]

39. Sharma, H.K.; Cervantes-lee, F.; Mahmoud, J.S.; Pannell, K.H. (Bis{2,4,6-Triisopropylphenyl}stannylene)Feroccenophane and Related Ring-Opened Products. *Organometallics* **1999**, *18*, 399–403. [CrossRef]

40. Weidenbruch, M.; Schäfers, K.; Pohl, S.; Saak, W.; Peters, K.; von Schnering, H.G. Verbindungen Des Germaniums Und Zinns II *. Bildung Und Strukturen Isomerer "Dichlordisupermesitylstannane.". *J. Organomet. Chem.* **1988**, *346*, 171–180. [CrossRef]

41. Available online: https://www.ccdc.cam.ac.uk (accessed on 14 February 2020).

42. Ahmad, S.U.; Beckmann, J.; Duthie, A. New Insights into the Formation and Reactivity of Molecular Organostannonic Acids. *Chem. Asian J.* **2010**, *5*, 160–168. [CrossRef]

43. Johnson, B.P.; Almstätter, S.; Dielmann, F.; Bodensteiner, M.; Scheer, M. Synthesis and Reactivity of Low-Valent Group 14 Element Compounds. *Z. Anorg. Allg. Chem.* **2010**, *636*, 1275–1285. [CrossRef]

44. Zeppek, C. Amine Base Induced Polymerization of Aryltin Hydrides: Mechanistic Insights & Nanomaterial Characterization. Ph.D. Thesis, Graz University of Technology, Graz, 2015.

45. Schittelkopf, K.; Fischer, R.C.; Meyer, S.; Wilfling, P.; Uhlig, F. Catalytic Dehydrogenative Coupling of Diorganotindihydrides by Lanthanide Diamide Complexes†. *Appl. Organomet. Chem.* **2010**, *24*, 897–901. [CrossRef]

46. Sindlinger, C.P.; Stasch, A.; Bettinger, H.F.; Wesemann, L. A Nitrogen-Base Catalyzed Generation of Organotin(Ii) Hydride from an Organotin Trihydride under Reductive Dihydrogen Elimination. *Chem. Sci.* **2015**, *6*, 4737–4751. [CrossRef] [PubMed]

47. Berthon-Gelloz, G.; Siegler, M.A.; Spek, A.L.; Tinant, B.; Reek, J.N.H.; Markó, I.E. IPr* an Easily Accessible Highly Hindered N-Heterocyclic Carbene. *Dalton Trans.* **2010**, *39*, 1444–1446. [CrossRef] [PubMed]

48. Blessing, R.H. An Empirical Correction for Absorption Anisotropy. *Acta Crystallogr. Sect. A* **1995**, *A51*, 33–38. [CrossRef] [PubMed]

49. Sheldrick, G.M. *SADABS Version 2.10 Siemens Area Detector Correction.*; Universitaet Goettingen: Goettingen, Germany, 2003.

50. Sheldrick, G.M. *SHELXTL Version 6.1.* Bruker AXS, Inc.: Wisconsin, WI, USA,, 2002.

51. Sheldrick, G.M. *GM SHELXS97 and SHELXL97*; Universitaet Goettingen: Goettingen, Germany, 2002.
52. Dolomanov, O.V.; Bourhis, L.J.; Gildea, R.J.; Howard, J.A.K.; Puschmann, H. OLEX2: A Complete Structure Solution, Refinement and Analysis Program. *J. Appl. Crystallogr.* **2009**, *42*, 339–341. [CrossRef]
53. Spek, A.L. Single-Crystal Structure Validation with the Program PLATON. *J. Appl. Crystallogr.* **2003**, *36*, 7–13. [CrossRef]
54. Spek, A.L. Structure Validation in Chemical Crystallography. *Acta Crystallogr. Sect. D Biol. Crystallogr.* **2009**, *65*, 148–155. [CrossRef]

Sample Availability: Samples of the compounds are not available from the authors.